

1 Temperature control as key factor for optimal biohydrogen
2 production from thermomechanical pulping wastewater
3
4

5 *Paolo Dessì^{a,*}, Estefania Porca^b, Aino-Maija Lakaniemi^a, Gavin Collins^b, Piet N. L. Lens^{a,c}*
6

7 *^a Tampere University of Technology, Faculty of Natural Sciences, P.O. Box 541, FI-33101*

8 *Tampere, Finland*

9 *^bMicrobial Communities Laboratory, School of Natural Sciences, National University of Ireland*

10 *Galway, University Road, Galway, H91 TK33, Ireland*

11 *^cUNESCO-IHE, Institute for Water Education, Westvest 7, 2611AX Delft, The Netherlands*
12

13 Manuscript submitted to: *Biochemical Engineering Journal*
14

15 *Corresponding author: Phone: +39 3897651830, e-mail: paolo.dessi@tut.fi, mail: Tampere

16 University of Technology, P.O. Box 541, FI-33101 Tampere, Finland

17 Estefania Porca: estefania.porca@gmail.com

18 Aino-Maija Lakaniemi: aino-maija.lakaniemi@tut.fi

19 Gavin Collins: gavin.collins@nuigalway.ie

20 Piet N.L. Lens: piet.lens@tut.fi
21
22

23 **Abstract**

24 This study evaluates the use of non-pretreated thermo-mechanical pulping (TMP) wastewater as a
25 potential substrate for hydrogen production by dark fermentation. Batch incubations were
26 conducted in a temperature gradient incubator at temperatures ranging from 37 to 80 °C, using an
27 inoculum from a thermophilic, xylose-fed, hydrogen-producing fluidised bed reactor. The aim was
28 to assess the short-term response of the microbial communities to the different temperatures with
29 respect to both hydrogen yield and composition of the active microbial community. High
30 throughput sequencing (MiSeq) of the reversely transcribed 16S rRNA showed that
31 *Thermoanaerobacterium* sp. dominated the active microbial community at 70 °C, resulting in the
32 highest hydrogen yield of 3.6 (\pm 0.1) mmol H₂ g⁻¹ COD_{tot} supplied. Lower hydrogen yields were
33 obtained at the temperature range from 37 to 65 °C, likely due to consumption of the produced
34 hydrogen by homoacetogenesis. No hydrogen production was detected at temperatures above 70
35 °C. Thermomechanical pulping wastewaters are released at high temperatures (50 to 80 °C), and
36 thus dark fermentation at 70 °C could be sustained using the heat produced by the pulp and paper
37 plant itself without any requirement for external heating.

38

39 **Keywords**

40 Dark fermentation, MiSeq, Pulp and paper mill wastewater, *Thermoanaerobacterium*,
41 Thermomechanical pulping, Thermophilic

42

43

44

45

46

47

48

49 **1. Introduction**

50 Pulp and paper industry is facing an economic challenge due to globalised competition and
51 decreasing paper demand (Machani et al., 2014). The long-term success of the industry is believed
52 to be strictly linked to the ability of companies to innovate and create new value streams, which are
53 predicted to generate 40% of the companies' turnover in 2030 (Toppinen et al., 2017). A biorefinery
54 concept, in which waste from the pulp and paper making process is used as a resource to generate
55 value-added products such as biofuels and biochemicals, is a promising strategy to expand the
56 product platform, reduce waste disposal costs and fulfil the environmental regulations on waste
57 emissions (Kinnunen et al., 2015; Machani et al., 2014; Moncada B. et al., 2016).

58

59 Pulping is the major source of polluted wastewaters of the whole papermaking process (Pokhrel and
60 Viraraghavan, 2004). Pulp mill wastewater is typically treated by the traditional activated sludge
61 process, but anaerobic processes have the advantages of coupling wastewater treatment to
62 renewable energy production, produce a lower quantity of waste sludge and require a smaller
63 volume than aerobic processes (Ashrafi et al., 2015). Among pulping processes, thermomechanical
64 pulping (TMP) produces a wastewater more suited for anaerobic biological processes than
65 chemical-based pulping, due to the low concentrations of inhibitory compounds such as sulphate,
66 sulphite, hydrogen peroxide, resin acid and fatty acids (Ekstrand et al., 2013; Rintala and Puhakka,
67 1994).

68

69 Thermomechanical pulping wastewater has been successfully used as a substrate for both
70 mesophilic (Gao et al., 2016) and thermophilic (Rintala and Lepistö, 1992) methane production via
71 anaerobic digestion. However, hydrogen (H₂) is a carbon free fuel expected to play a pivotal role in
72 energy production in the future (Boodhun et al., 2017). Dark fermentative H₂ production has the
73 potential for energy recovery from waste paper hydrolysate (Eker and Sarp, 2017), pulp and paper
74 mill effluent hydrolysates (Lakshmidēvi and Muthukumar, 2010) and even from untreated pulps

75 (Nissilä et al., 2012). Dark fermentative H₂ production has also been reported from carbohydrate-
76 containing wastewaters, such as starch wastewater and palm oil mill effluent (Badiei et al., 2011;
77 Xie et al., 2014). Although TMP wastewaters are characterized by a high content of carbohydrates
78 (25 to 40% of the total COD) (Rintala and Puhakka, 1994), to our knowledge it has not yet been
79 tested as a substrate for H₂ dark fermentation.

80

81 Thermophilic dark fermentation of TMP wastewater could be advantageous, as both biological
82 polysaccharide hydrolysis (Elsharnouby et al., 2013) and H₂ yielding reactions (Verhaart et al.,
83 2010) are favoured by high temperature. High temperature also limits the growth of
84 homoacetogenic bacteria and methanogenic archaea (Oh et al., 2003), which may consume the
85 produced H₂ in mixed culture systems. The main drawback of thermophilic processes is the energy
86 required to heat the reactors, but TMP wastewaters are released from the pulping process at a
87 temperature of 50 to 80 °C (Rintala and Lepistö, 1992), and could therefore be treated in
88 thermophilic bioreactors with minimal, or even without external heating.

89

90 Temperature is a key factor in dark fermentation, as even a change of a few degrees may result in
91 the development of a different microbial community and thus, affect the H₂ yield (Dessi et al.,
92 2018; Karadag and Puhakka, 2010). Understanding of the composition of the microbial community
93 is also crucial in order to optimize the complex microbial H₂ production process, involving both
94 hydrolytic and fermentative microorganisms (Kumar et al., 2017). Microbial communities from
95 dark fermentation of lignocellulose-based waste and wastewaters have been previously studied at
96 DNA level (Nissilä et al., 2012; Xie et al., 2014), but a RNA-based approach can provide more
97 detailed information on the microorganisms that produce (and consume) H₂. Furthermore, the time
98 response on RNA changes is much faster than on DNA changes (De Vrieze et al., 2016), allowing
99 to detect the response of the microbial community to an environmental change in a relatively short
100 time.

101

102 In a previous study, a mixed culture was successfully adapted to thermophilic (70 °C) dark
103 fermentation of xylose in a fluidised bed reactor (FBR) and the H₂ producing
104 *Thermoanaerobacterium* sp. accounted for > 99% of the active microbial community (Dessi et al.,
105 2018). In this study, the same adapted mixed culture was used to test if TMP wastewater is a
106 suitable substrate for dark fermentative H₂ production at various temperatures (from 37 to 80 °C),
107 and to describe how the active microbial community responds to the different temperatures.

108

109 **2. Materials and methods**

110 ***2.1 Source of microorganisms***

111 The inoculum used in this study was biofilm-coated activated carbon originating from a
112 thermophilic fluidised bed reactor (FBR) used to study H₂ production from xylose via dark
113 fermentation by gradually increasing the temperature of the reactor from 55 to 70 °C (Dessi et al.,
114 2018). The FBR was initially inoculated with heat-treated (90 °C, 15 min) activated sludge
115 originating from a municipal wastewater treatment plant (Viinikanlahti, Tampere, Finland). The
116 biofilm-coated activated carbon granules were sampled after 185 days of reactor operation, at that
117 point the FBR had been operated at 70 °C for 27 days. No xylose was present in the FBR medium at
118 the sampling time. The granules were stored at 4 °C for one week prior to utilisation. This inoculum
119 was used because the microbial community was dominated by *Thermoanaerobacterium* sp. (Dessi
120 et al., 2018), which previously showed potential for hydrolysis of lignocellulosic substrates and H₂
121 production from the resulting sugars (Cao et al., 2014).

122

123 ***2.2 Wastewater characterization***

124 The wastewater was collected from a pulp and paper mill located in Finland. It was the effluent of a
125 TMP process, in which wood was exposed to a high-temperature (120 °C) steam in order to obtain
126 the pulp. The wastewater had a temperature of about 70 °C at the time of the sampling, but was

127 cooled down and stored at 4 °C to minimise biological activity that might affect its composition.
128 The wastewater had a pH of 5.0 and a composition as given in Table 1.

129

130 [Table 1 here](#)

131

132 ***2.3 Temperature-gradient batch set-up***

133 The batch cultures were conducted in anaerobic tubes with a total volume of 26 mL (17 mL
134 working volume and 9 mL headspace). The tubes were inoculated by adding 2 mL of biofilm-
135 coated activated carbon granules to 15 mL of TMP wastewater (Table 1). All the tubes were flushed
136 with N₂ for 5 min, and the internal pressure was equilibrated to atmospheric pressure by removing
137 the excess gas using a syringe and a needle before incubation. The initial pH of the batch cultures
138 (wastewater and inoculum) was adjusted to 6.3 (± 0.1) using 1 M NaOH, as higher pH may favour
139 the growth of methanogenic archaea (Jung-Yeol et al., 2012). The tubes were incubated at 200 rpm
140 shaking in a temperature-gradient incubator (Test Tube Oscillator, Terratec Asia Pacific, Australia) at
141 37, 42, 48, 55, 59, 65, 70, 74 or 80°C (duplicate tubes at each temperature). The experiment was
142 interrupted after 111 hours, when no H₂ production was detected in any of the vials in two
143 consecutive samples, as long inactive periods may affect the RNA-level analysis (De Vrieze et al.,
144 2016).

145

146 Gas samples were collected for analysis 1 to 3 times per day. End-point liquid samples were
147 collected and stored at -20 °C before analysis. Non-inoculated control incubations, with fresh
148 activated carbon and TMP wastewater, were prepared at 37, 55 and 70 °C. Control incubations
149 containing 2 mL of fresh activated carbon and a mix of acetate and butyrate in Milli-Q® water (0.86
150 g COD_{tot} L⁻¹ each, 15 mL volume) were also prepared at 42, 65 and 80 °C to assess possible
151 adsorption of VFAs on virgin activated carbon.

152

153 **2.4 Microbial community analyses**

154 Biofilm-coated activated carbon granules and liquid medium were collected at the end of the
155 experiment and stored in 5 mL Eppendorf tubes at -80 °C. Microbial community analysis was
156 conducted separately on microbial communities growing attached to the granules and suspended in
157 the liquid medium, as the growth of suspended biomass was clearly visible in the vials after
158 incubation in the temperature range from 42 to 59 °C. Nucleic acids extraction using a modified
159 method from Griffiths et al. (2000), DNA inhibition, complementary DNA (cDNA) synthesis and
160 sequencing (using an Illumina MiSeq platform) were performed as described previously (Dessi et
161 al., 2018). Sequence analysis (1,395,864 sequences in total, 1,238,862 after quality check) was also
162 performed according to Dessì et al. (2018), but using a more recent version of Mothur (v1.39.5) and
163 Silva database (v128). The Illumina sequencing data was deposited to the NCBI Sequence Read
164 Archive under BioProject Number PRJNA428338.

165

166 **2.5 Analytical methods**

167 Gas production in the tubes was quantified by a volumetric syringe method (Owen et al., 1979), and
168 the gas composition was determined by gas chromatography-thermal conductivity detector (GC-
169 TCD) as reported previously by Dessì et al. (2017). Acetate, butyrate, ethanol, propionate, lactate,
170 and formate concentrations were measured with a high-performance liquid chromatograph (HPLC)
171 equipped with a refractive index detector (RID) (Shimadzu, Japan) and a Rezex RHM-
172 monosaccharide column (Phenomenex, USA) held at 40 °C. The mobile phase was 5 mM H₂SO₄
173 and the flow rate was 0.6 mL min⁻¹. Glucose and xylose concentrations were measured using a
174 HPLC equipped with a RID and a RPM-monosaccharide column (Phenomenex, USA) held at 85 °C
175 with Milli-Q[®] water at a flow rate of 0.6 mL min⁻¹ as the mobile phase. Furfural concentrations
176 were measured by gas chromatography-mass spectrometry (GC-MS) according to Doddapaneni et
177 al. (2018). Samples for HPLC and GC-MS analysis were filtered using 0.2 µm pore size filters.
178 Total chemical oxygen demand (COD_{tot}) and COD of the soluble compounds (COD_s) was measured

179 using the dichromate method according to the Finnish standard SFS 5504. Initial and final pH of the
180 culture and the pH of the wastewater were determined using a WTW pH 330 meter equipped with a
181 Hamilton® Slimtrode probe (Sigma-Aldrich, USA). Total solids, volatile solids, total nitrogen and
182 $\text{PO}_4^{3-}\text{-P}$ were determined by the APHA standard procedures (APHA, 1998).

183

184 **2.6 Calculations**

185 Cumulative H_2 and CO_2 production was calculated according to Logan et al. (2002) and corrected
186 for temperature according to the Arrhenius equation. The theoretical COD_{tot} was estimated from the
187 sum of the compounds detected by HPLC, according to the following equation (Van Haandel and
188 Van der Lubbe, 2012):

189

$$190 \text{COD}_{\text{tot}} = 8 \cdot (4x + y - 2z) / (12x + y + 16z) \text{ g COD}_{\text{tot}} \text{ g}^{-1} \text{C}_x\text{H}_y\text{O}_z \quad (1)$$

191

192 where x, y and z are the number of C, H and O atoms in the organic molecule, respectively.

193

194 **2.7 Statistical analysis**

195 One-way analysis of variance (ANOVA) and the Tukey test (Box et al., 1978) at $p = 0.05$ were
196 conducted using the IBM SPSS Statistics package to assess significant differences in H_2 yield after
197 incubation at different temperatures.

198

199 **3. Results**

200 **3.1 Hydrogen production from TMP wastewater at the various temperatures**

201 Batch incubations with TMP wastewater resulted in a different net H_2 yield at different
202 temperatures (Figure 1; Table 2). The highest final H_2 yield of $3.6 (\pm 0.1) \text{ mmol H}_2 \text{ g}^{-1} \text{COD}_{\text{tot}}$ was
203 obtained in the batch cultures at 70°C , in which H_2 production started within 24 h of incubation and
204 remained stable after reaching the maximum (Figure 1). The maximum H_2 yield obtained at 65°C

205 was comparable to the one obtained at 70 °C, but the produced H₂ started to be consumed within 36
206 h resulting in a 51% lower final yield (Figure 1; Table 2). In the batch cultures at temperatures
207 lower than 70 °C, the H₂ produced was always partially (at 37, 42, 59 and 65 °C) or totally (at 48
208 and 55 °C) consumed. A negligible H₂ production was obtained at both 74 and 80 °C (Figure 1), as
209 well as in the non-inoculated control incubations (Figure S1 in Supplementary Material).

210

211 [Figure 1 here](#)

212

213 [Table 2 here](#)

214

215 ***3.2 COD_{tot} removal and metabolite production at the various temperatures***

216 Similarly to H₂ production yields, dark fermentation of TMP wastewater at the various temperatures
217 resulted in a different composition of the liquid phase (Figure 2). Acetate was the most abundant
218 metabolite detected in the temperature range from 37 to 70 °C. The final acetate concentration
219 increased with temperature from 0.34 (± 0.04) g COD_{tot} L⁻¹ at 37 °C to 0.75 (± 0.18) g COD_{tot} L⁻¹ at
220 55 °C, and then decreased stepwise to 0.07 (± 0.00) and 0.08 (± 0.01) g COD_{tot} L⁻¹ at 74 and 80 °C,
221 respectively (Figure 2). Butyrate was found regardless of the incubation temperature, with a final
222 concentration ranging from 0.06 (± 0.00) g COD_{tot} L⁻¹ at 70 °C to 0.19 (± 0.00) g COD_{tot} L⁻¹ at 59
223 °C. Ethanol was produced at 37, 42, 59, 65 and 70 °C, with a maximum of 0.14 (± 0.02) g COD_{tot} L⁻¹
224 at 65 °C (Figure 2). Dark fermentation of TMP wastewater caused a pH decrease from the initial
225 value of 6.3: the final pH ranged from 5.7 to 6.1 after incubation at 42, 48, 55, 59, 74 and 80 °C, but
226 was only 5.5 (± 0.1) after incubation at 37 °C, 5.2 (± 0.1) at 65 °C and 5.3 (± 0.0) at 70 °C (Figure
227 2).

228

229 [Figure 2 here](#)

230

231 In the batch incubations at various temperatures, the COD_{tot} removal efficiency ranged from 69.4%
232 at 74 °C to 79.7% at 42 °C, resulting in a decrease from the initial concentration of 2.86 (± 0.00) g
233 COD_{tot} L⁻¹ to a final concentration ranging from 0.58 (± 0.23) g COD_{tot} L⁻¹ at 42 °C and 0.88 (±
234 0.06) g COD_{tot} L⁻¹ at 74 °C (Table 3). The COD_{tot} removal efficiency was likely overestimated due
235 to the adsorption of VFAs on the activated carbon: in the adsorption experiment (Figure S2 in
236 Supplementary Material), up to 27% of the acetate and 90% of the butyrate was, in fact, adsorbed
237 on the fresh activated carbon after 111 h of incubation. The COD_{tot} measured was comparable to the
238 COD_{tot} estimated (using Eq. 1) by the sum of sugars and volatile fatty acids in the liquid phase after
239 incubation in the temperature range from 42 to 65 °C (Table 3) . However, the difference between
240 measured and estimated COD_{tot} was about 0.20 g COD_{tot} L⁻¹ at 37, 70 and 80 °C, and even higher at
241 74 °C (0.51 g COD_{tot} L⁻¹).

242

243 [Table 3 here](#)

244

245 **3.3 Effect of temperature on the active microbial community**

246 Incubation temperature clearly affected the composition of the active microbial communities
247 growing for 111 h on TMP wastewater (Figure 3, Table 4). At 37 °C, *Clostridium* sp. accounted for
248 84 and 90% of the attached and suspended active microbial community, respectively. Higher
249 temperature resulted in a gradual decrease of the relative abundance of *Clostridium* sp., being 54%
250 of the attached active microbial community and < 2% of the suspended active microbial community
251 after incubation at 55 °C (Figure 3). *Clostridium* sp. was not detected either in the attached or
252 suspended active community after incubation at temperatures ≥ 59 °C (Figure 3). A bacterium
253 belonging to the order of *Bacillales* closely related to *B. coagulans* (Table 4) was detected in the
254 active attached and suspended microbial communities after incubation at 42 °C, with a relative
255 abundance of 14 and 10%, respectively, and only in suspended form after incubation at 48 °C, with
256 a relative abundance of 50% (Figure 3).

257

258 The relative abundance of *Thermoanaerobacterium* sp. (99% similarity to *T.*
259 *thermosaccharolyticum*) among the attached active microorganisms gradually increased with
260 temperature, being only 2% after incubation at 37 °C and 87% at 59 °C (Figure 3, Table 4).
261 *Thermoanaerobacterium* sp. was also the most common suspended active microorganism after
262 incubation at 55 and 59 °C, with a relative abundance of 96 and 83%, respectively. After incubation
263 at 65 °C, the relative abundance of *Thermoanaerobacterium* sp. in the attached and suspended
264 active microbial community decreased to 57 and 25%, respectively, whereas unclassified
265 *Firmicutes*, with 92% similarity to *Calditerricola* sp. (Table 4) were found with a relative
266 abundance of 30 and 28%, respectively. After incubation at 70 °C, *Thermoanaerobacterium* sp. was
267 again the dominant active microorganism in both attached and suspended form, with a relative
268 abundance of 88 to 89%. After incubation at 59 and 70 °C, *Caldanaerobius* sp. was also found in
269 both attached and suspended form with relative abundance below 10% (Figure 3). After incubation
270 at both 74 and 80 °C, the RNA concentration was not high enough to perform the analysis due to
271 poor microbial growth, and thus microbial communities from 74 and 80 °C could not be analysed.

272

273 Figure 3 here

274

275 Table 4 here

276

277 **4. Discussion**

278 ***4.1 Fermentation of TMP wastewater at different temperatures***

279 Hydrogen production from TMP wastewater inoculated with biofilm-coated activated carbon
280 granules was observed at a wide temperature range from 37 to 70 °C (Figure 1). The highest final
281 H₂ yield of 3.6 (± 0.1) mmol H₂ g⁻¹ COD_{tot} supplied, or 4.9 mmol H₂ g⁻¹ COD_{tot} consumed, was
282 obtained at 70 °C (Table 2), which could be expected as the inoculum was collected from an FBR

283 operated at 70 °C (Dessì et al., 2018). The H₂ yield obtained in this study is of the same order of
284 magnitude compared to previous studies on thermophilic direct dark fermentation of industrial,
285 sugar-containing wastewaters. For example, Xie et al. (2014) obtained 5.8 mmol H₂ g⁻¹ COD_{tot} from
286 starch wastewater at 55°C by a mixed culture dominated by *T. thermosaccharolyticum*, whereas
287 Khongkliang et al. (2017) obtained 11.4 mmol H₂ g⁻¹ COD_{tot} from starch wastewater by a pure
288 culture of *T. thermosaccharolyticum*.

289

290 The thermophilic active mixed microbial community previously enriched on xylose in the FBR was
291 dominated by microorganisms closely related to *Thermoanaerobacterium thermosaccharolyticum*
292 (Dessì et al., 2018). Changing of the substrate from xylose to TMP wastewater marginally impacted
293 the active microbial community in the temperature range 59 to 70 °C, as most of the sequences
294 obtained from the RNA samples matched *T. thermosaccharolyticum* (Table 4). A mixed culture
295 dominated by *T. thermosaccharolyticum* has been shown to produce 7 mmol H₂ g⁻¹ cellulose at 70
296 °C (Gadow et al., 2013), showing potential for the one-step conversion of lignocellulosic materials
297 to H₂, avoiding a costly hydrolysis step. In fact, the genus *Thermoanaerobacterium* includes strains
298 of cellulolytic microorganisms, such as some strains of *T. thermosaccharolyticum*, able to hydrolyse
299 both cellulose and hemicellulose, and produce H₂ from the resulting monosaccharides (Cao et al.,
300 2014). In this study, however, the microbial community analysis conducted at genus level does not
301 allow to assess possible cellulolytic capabilities of the detected *Thermoanaerobacterium* sp.

302

303 Although the inoculum was enriched for dark fermentation at 70 °C, H₂ production at 70 °C
304 occurred only after 24 h of incubation (Figure 1). This is probably due to the handling of the
305 inoculum, which was stored at 4 °C for one week prior to being used for this experiment. Changes
306 in gene expression and DNA replication were shown to occur in *Thermoanaerobacter*
307 *tengcongensis* as response to a cold shock (Liu et al., 2014), as could be the case for the
308 *Thermoanaerobacterium* sp. dominating the active microbial community of the inoculum used in

309 this study. Although *Thermoanaerobacterium* sp. was the most abundant microorganism (relative
310 abundance close to 90%) in both the attached and suspended microbial community at both 59 and
311 70 °C, its relative abundance was lower at 65 °C (Figure 3). The same phenomenon was observed in
312 the FBR from where the inoculum originated (Dessì et al., 2018), and was attributed to either the
313 decreased activity of *Thermoanaerobacterium* sp. or to the increased activity of competing
314 microorganisms at 65 °C.

315

316 Despite the inoculum was enriched for thermophilic dark fermentation, H₂ was already produced
317 after 12 h of incubation at 37 °C, reaching a maximum yield of 3.2 (± 0.1) mmol H₂ g⁻¹ COD_{tot}
318 supplied within 24 h (Figure 1). A maximum yield of only 0.9 mmol H₂ g⁻¹ COD_{tot} supplied was
319 previously obtained at 37 °C from a paper mill wastewater (production process type and wastewater
320 fraction used not specified) using heat treated digested sludge as inoculum (Marone et al., 2017).
321 The H₂ yields obtained in this study are also higher than those reported by Lucas et al. (2015) by
322 mesophilic (37 °C) dark fermentation of cassava, dairy and citrus wastewaters, which produced 1.4,
323 1.7 and 1.3 mmol H₂ g⁻¹ COD_{tot} supplied, respectively. This confirms the potential of TMP
324 wastewater for dark fermentation.

325

326 *Clostridium* sp. proliferated at 37 °C accounting for more than 80% of both the attached and
327 suspended active microbial community at the end of the batch incubation (Figure 3). It is plausible
328 that *Clostridium* sp. were present in the parent activated sludge but inactive in the FBR operated at
329 70 °C (Dessì et al., 2018). In fact, *Clostridium* spp. produce spores to survive under harsh
330 conditions, and are able to restore their metabolic activity after desporulation as soon as the
331 environmental conditions become more favourable (Li and Fang, 2007). *Clostridium* sp. cells might
332 also have been present in the TMP wastewater, which was not sterilised. However, the absence of
333 H₂ and CO₂ in the non-inoculated control incubation at 37 °C (Figure S1 in Supplementary
334 Material) suggests that *Clostridium* sp. did not proliferate in the absence of the inoculum.

335

336 In this study, no H₂ was produced at 74 or 80 °C (Figure 1) and the RNA concentration was too low
337 to allow sequencing analysis, suggesting a lack of active species. This was attributed to the source
338 of inoculum used, as species within the *Thermoanaerobacterium* genus, such as *T.*
339 *thermosaccharolyticum*, may be inhibited by temperatures higher than 70 °C (Ren et al., 2008).
340 Gadow et al. (2013) obtained H₂ production from cellulose by a mixed microflora from a sewage
341 sludge digester even at 75 and 80 °C. However, H₂ production at such high temperatures was
342 attributed to *Thermoanaerobacter tengcongensins* (Gadow et al., 2013), which was not part of the
343 active microbial community in this study. Some degradation products of hemicellulose such as
344 furfural or hydromethylfurfural may inhibit fermentative microorganisms (Jönsson et al., 2013),
345 including *Thermoanaerobacterium*, at a concentration over 1 g L⁻¹ (Cao et al., 2010). However, the
346 TMP process is conducted at temperatures below 120 °C, which is too low to produce such high
347 concentrations of these inhibitory compounds (Baêta et al., 2017). In fact, the concentration of
348 furfural in the TMP wastewater used in this study was below the detection limit of the GC-MS
349 (Table 1).

350

351 A decrease in the cumulative H₂ production occurred in all the incubations at temperatures lower
352 than 70 °C (Figure 1), probably due to the activity of homoacetogenic bacteria. Homoacetogenesis,
353 in which 4 moles of H₂ and 2 mol of CO₂ are consumed per mol of acetate produced, often occurs
354 in batch H₂ production experiments within the first 80 h of incubation, especially under mesophilic
355 conditions (for a review, see Saady, 2013). However, in this study, H₂ seems to be consumed faster
356 under thermophilic (from 48 to 65 °C) as compared to mesophilic (37 °C) conditions (Figure 1),
357 suggesting that homoacetogenic microorganisms were mainly thermophiles or moderate
358 thermophiles. The CO₂ concentration in the batch incubations did not decrease as expected in case
359 of homoacetogenesis (Figure S3 in Supplementary Material). However, this could be explained
360 considering that CO₂ production may occur also through non-hydrogenic pathways, mainly the

361 ethanol production pathway (Figure 2). In the non-inoculated control incubations, CO₂ was also
362 detected, together with acetate, at both 55 and 70 °C, where H₂ production was not observed (Figure
363 S1 in Supplementary Material). This suggests that non-hydrogenic, CO₂ producing pathways other
364 than ethanol production could have occurred as well.

365

366 Homoacetogens are among the most phylogenetically diverse functional groups of bacteria (Drake
367 et al., 2006). Among the thermophiles, *Moorella thermoacetica*, which accounted for 5% of the
368 suspended active community at 55 °C and 6% of the attached active community at 65 °C (Figure 3),
369 is a known homoacetogenic bacterium with an optimum growth temperature ranging from 55 to 60
370 °C (Drake et al., 2006). *Clostridium* spp. have also been previously found in thermophilic
371 fermentative reactors and associated with homoacetogenesis (Ryan et al., 2008). It is plausible that
372 the shift to autotrophic metabolism (e.g. homoacetogenesis) occurred after substrate depletion, as
373 suggested by Oh et al. (2003).

374

375 **4.2 COD_{tot} balance and metabolite production**

376 The COD_{tot} measured in the beginning of the incubations (Table 3) was 15% lower than the value
377 obtained while characterizing the TMP wastewater (Table 1). Apparently, some biological or non-
378 biological reaction occurred while storing the TMP wastewater at 4 °C before the experiment,
379 resulting in a slight COD_{tot} concentration decrease. The COD_{tot} removal efficiency during the
380 incubations was 69 to 80% regardless the incubation temperature (Table 3). It is in line with the
381 COD_{tot} removal from anaerobic digestion of pulp and paper wastewater reported in the literature
382 (Meyer and Edwards, 2014), but higher than expected for dark fermentation which usually removes
383 only 30 to 40% of the COD_{tot} (Sharma and Li, 2010). This was likely due to the adsorption of VFAs
384 on the activated carbon (Figure S2 in Supplementary Material), which caused an overestimation of
385 the COD_{tot} removal. However, it should be noted that the adsorption experiment (Figure S2 in
386 Supplementary Material) was performed with fresh activated carbon, whereas the main experiment

387 was conducted with biofilm-covered activated carbon. The latter could have been partially saturated
388 with VFAs at the moment of inoculation, as VFAs were also produced in the FBR from where the
389 inoculum originated (Dessi et al., 2018).

390

391 In the temperature range from 42 to 65 °C, more than 85% of the residual COD_{tot} was detected as
392 acetate, butyrate or ethanol by HPLC analysis (Table 3). However, 30 to 37% of the residual COD_{tot}
393 was not detected as compounds identified by HPLC analysis after incubation at 37, 70 and 80 °C,
394 and even 58% of the residual COD_{tot} was not identified after incubation at 74 °C. At 74 and 80 °C,
395 most of the undetected COD_{tot} was likely constituted by polysaccharides such as cellulose, which
396 were not degraded due to the lack of bacterial activity at such high temperatures. At 74 and 80 °C,
397 CO₂ was also not produced (Figure S3 in Supplementary Material), supporting this conclusion.
398 Lignin, which accounts for 16-49% of the COD_{tot} in TMP wastewater (Rintala and Puhakka, 1994)
399 can release VFAs at temperatures around 80 °C (Veluchamy and Kalamdhad, 2017), suggesting that
400 the acetate and butyrate detected at 74 and 80 °C (Figure 2) were produced physically rather than
401 biologically.

402

403 The simultaneous production of acetate and butyrate suggests that H₂ was produced via both the
404 acetate and butyrate pathway in the temperature range from 37 to 70 °C. Acetate was the main
405 metabolite found in the liquid phase at all temperatures tested, excluding 74 and 80 °C (Figure 2),
406 and was associated either to H₂ production through the acetate dark fermentative pathway or H₂
407 consumption by homoacetogenesis. Interestingly, acetate production increased with temperature in
408 the range from 37 to 55 °C, and then decreased stepwise at temperatures above 55 °C (Figure 2). In
409 particular, the high (> 0.7 g COD_{tot} L⁻¹) acetate (Figure 2) and concomitant low (< 0.5 mmol g⁻¹
410 COD_{tot}) cumulative H₂ yield (Figure 1) suggest that the optimum growth temperature for
411 homoacetogenic bacteria was about 55 °C in this study. At 70 °C, however, the H₂ produced was

412 not consumed during the incubation (Figure 1), suggesting inhibition of homoacetogenic
413 microorganisms.

414

415 Solventogenesis occurred both in mesophilic (37 and 42 °C) and thermophilic (59, 65, and 70 °C)
416 batch cultures, resulting in ethanol production (Figure 2). *Clostridium* sp., which dominated the
417 active microbial communities under mesophilic conditions (Figure 3), may shift its metabolism
418 from acidogenesis to solventogenesis as response to a change of pH or volatile fatty acids
419 concentration, but the mechanism which triggers solventogenesis is not well understood (Kumar et
420 al., 2013). A pure culture of *T. thermosaccharolyticum* has been reported to produce ethanol
421 together with acetate and butyrate by dark fermentation of cellulose and complex lignocellulosic
422 substrates such as corn cob, corn straw and wheat straw (Cao et al., 2014). Similarly, in this study,
423 acetate, butyrate and ethanol were the main metabolites (Figure 2) of the dark fermentation of TMP
424 wastewater at 65 and 70 °C by a mixed culture dominated by *T. thermosaccharolyticum* (Figure 3;
425 Table 4).

426

427 **4.3 Practical implications**

428 Hydraulic retention times lower than 24 hours are typically used for dark fermentation of
429 wastewater in bioreactors operated in continuous mode (Lin et al., 2012). Therefore, based on the
430 results obtained in this batch experiment (Figure 1), dark fermentation of TMP wastewater at 37 and
431 65 °C appears favourable if suspended biomass bioreactors are used, as homoacetogenic bacteria
432 would be flushed out (Figure 1). However, bioreactors retaining high active biomass content, such
433 as FBRs or upflow anaerobic sludge bioreactors (UASBs), would enable higher organic loadings
434 and conversion rates than suspended biomass bioreactors (Koskinen et al., 2006). Therefore,
435 attached biomass bioreactors operated in continuous mode at 70 °C are recommended for H₂
436 production via dark fermentation of TMP wastewater. A proper insulation and temperature control
437 are nevertheless necessary to keep the temperature inside the bioreactor accurately at 70 °C, as a

438 decrease of 5 °C may already result in a decreased efficiency due to H₂ consumption by
439 homoacetogenic bacteria. However, H₂ production at 70 °C can be quickly restored in case of
440 failure of the temperature control. In fact, H₂ production was detected at 70 °C within only 24 h
441 (Figure 1) with a thermophilic inoculum previously stored at 4 °C for one week.

442

443 Despite the surprisingly high COD_{tot} removal efficiency of 69 to 80 % obtained in this study (Table
444 3), dark fermentation of TMP wastewater resulted in the generation of an effluent containing 0.5 to
445 1.0 g COD_{tot} L⁻¹ (Table 3), mainly in the form of VFAs, thus requiring further treatment prior
446 discharge to the environment. Such effluent can be either treated by a traditional activated sludge
447 plant, or further valorised by producing energy or high value chemicals. Promising strategies for the
448 valorisation of dark fermentation effluents include further H₂ production by photofermentation or
449 microbial electrolysis cells, methane production by anaerobic digestion, and bioplastics or
450 electricity production using microbial fuel cells (for reviews, see Ghimire et al., 2015 and Bundhoo,
451 2017).

452

453 **5. Conclusions**

454 Hydrogen was produced by dark fermentation from TMP wastewater at a wide range of
455 temperatures (37 to 70 °C) using a mixed microbial community enriched on xylose at thermophilic
456 conditions. An operation temperature of 70 °C was the most favourable for dark fermentative H₂
457 production and effectively repressed the activity of homoacetogenic bacteria. Therefore,
458 considering that TMP wastewater is produced at elevated temperature, dark fermentation at 70 °C
459 may be a cost-effective approach for the treatment and valorisation of this wastewater. However,
460 temperature must be efficiently controlled, as a shift of only a few degrees may decrease the H₂
461 yield.

462

463 **Acknowledgements**

464 This work was supported by the Marie Skłodowska-Curie European Joint Doctorate (EJD) in
465 Advanced Biological Waste-To-Energy Technologies (ABWET) funded from Horizon 2020 under
466 grant agreement no. 643071.

467

468 **References**

- 469 APHA, 1998. Standard Methods for the Examination of Water and Wastewater, twentieth ed.
470 American Public Health Association/American Water Works Association/Water Environment
471 Federation, Washington DC.
- 472 Ashrafi, O., Yerushalmi, L., Haghighat, F., 2015. Wastewater treatment in the pulp-and-paper
473 industry: A review of treatment processes and the associated greenhouse gas emission. *J.*
474 *Environ. Manage.* 158, 146–157.
- 475 Badiei, M., Jahim, J.M., Anuar, N., Abdullah, S.R.S., 2011. Effect of hydraulic retention time on
476 biohydrogen production from palm oil mill effluent in anaerobic sequencing batch reactor. *Int.*
477 *J. Hydrogen Energy* 36, 5912–5919.
- 478 Baêta, B.E.L., Cordeiro, P.H. de M., Passos, F., Gurgel, V.A.L., de Aquino, S.F., Fdz-Polanco, F.,
479 2017. Steam explosion pretreatment improved the biomethanization of coffee husks.
480 *Bioresour. Technol.* 245, 66–72.
- 481 Boodhun, B.S.F., Mudhoo, A., Kumar, G., Kim, S.-H., Lin, C.-Y., 2017. Research perspectives on
482 constraints, prospects and opportunities in biohydrogen production. *Int. J. Hydrogen Energy*
483 42, 27471–27481.
- 484 Box, G.E.P., Hunter, W.G., Hunter, J.S., 1978. Statistics for experimenters: An introduction to
485 design, data analysis, and model building. John Wiley and sons.
- 486 Bundhoo, Z.M.A., 2017. Coupling dark fermentation with biochemical or bioelectrochemical
487 systems for enhanced bio-energy production: A review. *Int. J. Hydrogen Energy* 42, 26667–
488 26686.
- 489 Cao, G.-L., Zhao, L., Wang, A.-J., Wang, Z.-Y., Ren, N.-Q., 2014. Single-step bioconversion of

490 lignocellulose to hydrogen using novel moderately thermophilic bacteria. *Biotechnol. Biofuels*
491 7, 82.

492 Cao, G., Ren, N., Wang, A., Guo, W., Xu, J., Liu, B., 2010. Effect of lignocellulose-derived
493 inhibitors on growth and hydrogen production by *Thermoanaerobacterium*
494 *thermosaccharolyticum* W16. *Int. J. Hydrogen Energy* 35, 13475–13480.

495 De Vrieze, J., Regueiro, L., Props, R., Vilchez-Vargas, R., Jáuregui, R., Pieper, D.H., Lema, J.M.,
496 Carballa, M., 2016. Presence does not imply activity: DNA and RNA patterns differ in
497 response to salt perturbation in anaerobic digestion. *Biotechnol. Biofuels* 9, 244.

498 Dessì, P., Lakaniemi, A.-M., Lens, P.N.L., 2017. Biohydrogen production from xylose by fresh and
499 digested activated sludge at 37, 55 and 70 °C. *Water Res.* 115, 120–129.

500 Dessì, P., Porca, E., Waters, N.R., Lakaniemi, A.-M., Collins, G., Lens, P.N.L., 2018. Thermophilic
501 versus mesophilic dark fermentation in xylose-fed fluidised bed reactors: Biohydrogen
502 production and active microbial community. *Int. J. Hydrogen Energy* 43, 5473–5485.

503 Doddapaneni, T.R.K.C., Jain, R., Praveenkumar, R., Rintala, J., Romar, H., Konttinen, J., 2018.
504 Adsorption of furfural from torrefaction condensate using torrefied biomass. *Chem. Eng. J.*
505 334, 558–568.

506 Drake, H.L., Küsel, K., Matthies, C., 2006. Acetogenic Prokaryotes, in: Springer (Ed.), *The*
507 *Prokaryotes*. New York, pp. 354–420.

508 Eker, S., Sarp, M., 2017. Hydrogen gas production from waste paper by dark fermentation: Effects
509 of initial substrate and biomass concentrations. *Int. J. Hydrogen Energy* 42, 2562–2568.

510 Ekstrand, E.-M., Larsson, M., Truong, X.-B., Cardell, L., Borgström, Y., Björn, A., Ejlertsson, J.,
511 Svensson, B.H., Nilsson, F., Karlsson, A., 2013. Methane potentials of the Swedish pulp and
512 paper industry – A screening of wastewater effluents. *Appl. Energy* 112, 507–517.

513 Elsharnouby, O., Hafez, H., Nakhla, G., El Naggar, M.H., 2013. A critical literature review on
514 biohydrogen production by pure cultures. *Int. J. Hydrogen Energy* 38, 4945–4966.

515 Gadow, S.I., Jiang, H., Hojo, T., Li, Y.-Y., 2013. Cellulosic hydrogen production and microbial

516 community characterization in hyper-thermophilic continuous bioreactor. *Int. J. Hydrogen*
517 *Energy* 38, 7259–7267.

518 Gao, W.J., Han, M.N., Xu, C.C., Liao, B.Q., Hong, Y., Cumin, J., Dagnew, M., 2016. Performance
519 of submerged anaerobic membrane bioreactor for thermomechanical pulping wastewater
520 treatment. *J. Water Process Eng.* 13, 70–78.

521 Ghimire, A., Frunzo, L., Pirozzi, F., Trably, E., Escudie, R., Lens, P.N.L., Esposito, G., 2015. A
522 review on dark fermentative biohydrogen production from organic biomass: Process
523 parameters and use of by-products. *Appl. Energy* 144, 73–95.

524 Griffiths, R.I., Whiteley, A.S., O'Donnell, A.G., Bailey, M.J., 2000. Rapid method for coextraction
525 of DNA and RNA from natural environments for analysis of ribosomal DNA- and rRNA-
526 based microbial community composition. *Appl. Environ. Microbiol.* 66, 5488–5491.

527 Jung-Yeol, L., Chen, X.-J., Lee, E.-J., Min, K.-S., 2012. Effects of pH and carbon sources on
528 biohydrogen production by co-culture of *Clostridium butyricum* and *Rhodobacter sphaeroides*.
529 *J. Microbiol. Biotechnol.* 22, 400–406.

530 Jönsson, L.J., Alriksson, B., Nilvebrant, N.-O., 2013. Bioconversion of lignocellulose: inhibitors
531 and detoxification. *Biotechnol. Biofuels* 6, 16.

532 Karadag, D., Puhakka, J.A., 2010. Effect of changing temperature on anaerobic hydrogen
533 production and microbial community composition in an open-mixed culture bioreactor. *Int. J.*
534 *Hydrogen Energy* 35, 10954–10959.

535 Khongkliang, P., Kongjan, P., Utarapichat, B., Reungsang, A., O-Thong, S., 2017. Continuous
536 hydrogen production from cassava starch processing wastewater by two-stage thermophilic
537 dark fermentation and microbial electrolysis. *Int. J. Hydrogen Energy* 42, 27584–27592.

538 Kinnunen, V., Ylä-Outinen, A., Rintala, J., 2015. Mesophilic anaerobic digestion of pulp and paper
539 industry biosludge–long-term reactor performance and effects of thermal pretreatment. *Water*
540 *Res.* 87, 105–111.

541 Koskinen, P.E.P., Kaksonen, A.H., Puhakka, J.A., 2006. The relationship between instability of H₂

542 production and compositions of bacterial communities within a dark fermentation fluidized-
543 bed bioreactor. *Biotechnol. Bioeng.* 97, 742–758.

544 Kumar, G., Sivagurunathan, P., Sen, B., Mudhoo, A., Davila-Vazquez, G., Wang, G., Kim, S.-H.,
545 2017. Research and development perspectives of lignocellulose-based biohydrogen production.
546 *Int. Biodeterior. Biodegradation* 119, 225–238.

547 Kumar, M., Gayen, K., Saini, S., 2013. Role of extracellular cues to trigger the metabolic phase
548 shifting from acidogenesis to solventogenesis in *Clostridium acetobutylicum*. *Bioresour.*
549 *Technol.* 138, 55–62.

550 Lakshmidevi, R., Muthukumar, K., 2010. Enzymatic saccharification and fermentation of paper and
551 pulp industry effluent for biohydrogen production. *Int. J. Hydrogen Energy* 35, 3389–3400.

552 Li, C., Fang, H.H.P., 2007. Fermentative hydrogen production from wastewater and solid wastes by
553 mixed cultures. *Crit. Rev. Environ. Sci. Technol.* 37, 1–39.

554 Lin, C.-Y., Lay, C.-H., Sen, B., Chu, C.-Y., Kumar, G., Chen, C.-C., Chang, J.-S., 2012.
555 Fermentative hydrogen production from wastewaters: A review and prognosis. *Int. J.*
556 *Hydrogen Energy* 37, 15632–15642.

557 Liu, B., Zhang, Y., Zhang, W., 2014. RNA-seq-based analysis of cold shock response in
558 *Thermoanaerobacter tengcongensis*, a bacterium harboring a single cold shock protein
559 encoding gene. *PLoS One* 9, 3.

560 Logan, B.E., Oh, S.-E., Kim, I.S., Van Ginkel, S., 2002. Biological hydrogen production measured
561 in batch anaerobic respirometers. *Environ. Sci. Technol.* 36, 2530–2535.

562 Lucas, S.D.M., Peixoto, G., Mockaitis, G., Zaiat, M., Gomes, S.D., 2015. Energy recovery from
563 agro-industrial wastewaters through biohydrogen production: Kinetic evaluation and
564 technological feasibility. *Renew. Energy* 75, 496–504.

565 Machani, M., Nourelfath, M., D'Amours, S., 2014. A mathematically-based framework for
566 evaluating the technical and economic potential of integrating bioenergy production within
567 pulp and paper mills. *Biomass and Bioenergy* 63, 126–139.

568 Marone, A., Ayala-Campos, O.R., Trably, E., Carmona-Martínez, A.A., Moscoviz, R., Latrille, E.,
569 Steyer, J.-P., Alcaraz-Gonzalez, V., Bernet, N., 2017. Coupling dark fermentation and
570 microbial electrolysis to enhance bio-hydrogen production from agro-industrial wastewaters
571 and by-products in a bio-refinery framework. *Int. J. Hydrogen Energy* 42, 1609–1621.

572 Meyer, T., Edwards, E.A., 2014. Anaerobic digestion of pulp and paper mill wastewater and sludge.
573 *Water Res.* 65, 321–349.

574 Moncada B., J., Aristizábal M., V., Cardona A., C.A., 2016. Design strategies for sustainable
575 biorefineries. *Biochem. Eng. J.* 116, 122–134.

576 Nissilä, M.E., Li, Y.-C., Wu, S.-Y., Lin, C.-Y., Puhakka, J.A., 2012. Hydrogenic and methanogenic
577 fermentation of birch and conifer pulps. *Appl. Energy* 100, 58–65.

578 Oh, S.-E., Van Ginkel, S., Logan, B.E., 2003. The relative effectiveness of pH control and heat
579 treatment for enhancing biohydrogen gas production. *Environ. Sci. Technol.* 37, 5186–90.

580 Owen, W.F., Stuckey, D.C., Healy Jr., J.B., Young, L.Y., McCarty, P.L., 1979. Bioassay for
581 monitoring biochemical methane potential and anaerobic toxicity. *Water Res.* 13, 485–492.

582 Pokhrel, D., Viraraghavan, T., 2004. Treatment of pulp and paper mill wastewater—A review. *Sci.*
583 *Total Environ.* 333, 37–58.

584 Ren, N., Cao, G., Wang, A., Lee, D., Guo, W., Zhu, Y., 2008. Dark fermentation of xylose and
585 glucose mix using isolated *Thermoanaerobacterium thermosaccharolyticum* W16. *Int. J.*
586 *Hydrogen Energy* 33, 6124–6132.

587 Rintala, J.A., Lepistö, S.S., 1992. Anaerobic treatment of thermomechanical pulping whitewater at
588 35-70°C. *Water Res.* 26, 1297–1305.

589 Rintala, J.A., Puhakka, J.A., 1994. Anaerobic treatment in pulp- and paper-mill waste management:
590 A review. *Bioresour. Technol.* 47, 1–18.

591 Ryan, P., Forbes, C., Colleran, E., 2008. Investigation of the diversity of homoacetogenic bacteria
592 in mesophilic and thermophilic anaerobic sludges using the formyltetrahydrofolate synthetase
593 gene. *Water Sci. Technol.* 57, 675–680.

- 594 Saady, N.M.C., 2013. Homoacetogenesis during hydrogen production by mixed cultures dark
595 fermentation: Unresolved challenge. *Int. J. Hydrogen Energy* 38, 13172–13191.
- 596 Sharma, Y., Li, B., 2010. Optimizing energy harvest in wastewater treatment by combining
597 anaerobic hydrogen producing biofermentor (HPB) and microbial fuel cell (MFC). *Int. J.*
598 *Hydrogen Energy* 35, 3789–3797.
- 599 Toppinen, A., Pätäri, S., Tuppura, A., Jantunen, A., 2017. The European pulp and paper industry in
600 transition to a bio-economy: A Delphi study. *Futures* 88, 1–14.
- 601 Van Haandel, A., Van der Lubbe, J., 2012. *Handbook of biological wastewater treatment: Design*
602 *and Optimisation of Activated Sludge Systems*. Quist Publishing, Leidschendam, The
603 Netherlands.
- 604 Veluchamy, C., Kalamdhad, A.S., 2017. Enhancement of hydrolysis of lignocellulose waste pulp
605 and paper mill sludge through different heating processes on thermal pretreatment. *J. Clean.*
606 *Prod.* 168, 219–226.
- 607 Verhaart, M.R.A., Bielen, A.A.M., Van der Oost, J., Stams, A.J.M., Kengen, S.W.M., 2010.
608 Hydrogen production by hyperthermophilic and extremely thermophilic bacteria and archaea:
609 Mechanisms for reductant disposal. *Environ. Technol.* 31, 993–1003.
- 610 Xie, L., Dong, N., Wang, L., Zhou, Q., 2014. Thermophilic hydrogen production from starch
611 wastewater using two-phase sequencing batch fermentation coupled with UASB methanogenic
612 effluent recycling. *Int. J. Hydrogen Energy* 39, 20942–20949.

613

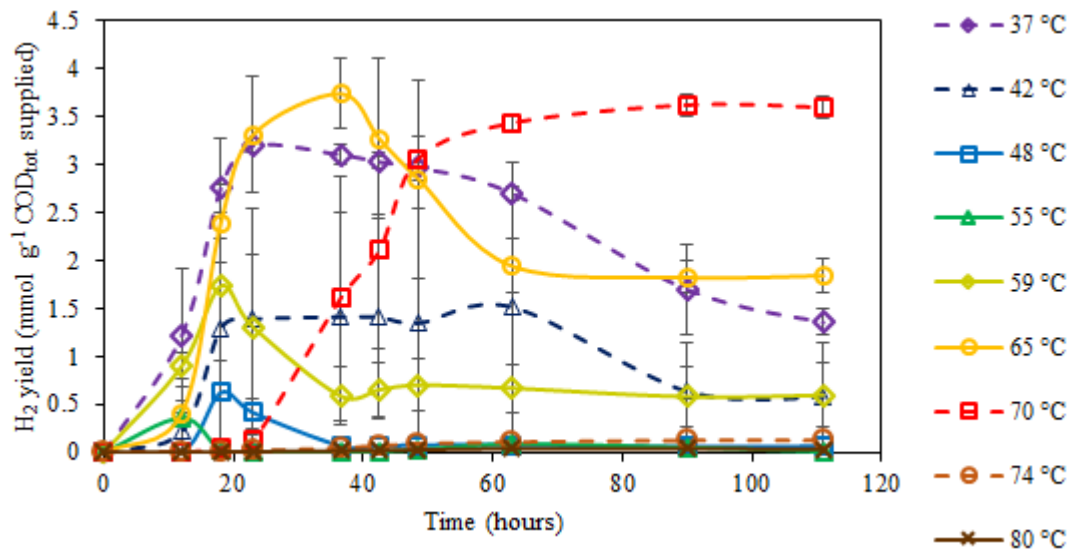
614

615

616

617 **Figures**

618 **Figure 1** – Hydrogen yield from batch incubation of thermomechanical pulping wastewater at
619 various temperatures (from 37 to 80 °C) using thermophilic biofilm-containing activated carbon as
620 inoculum. Error bars refer to the standard deviations of the duplicates.



621

622

623

624

625

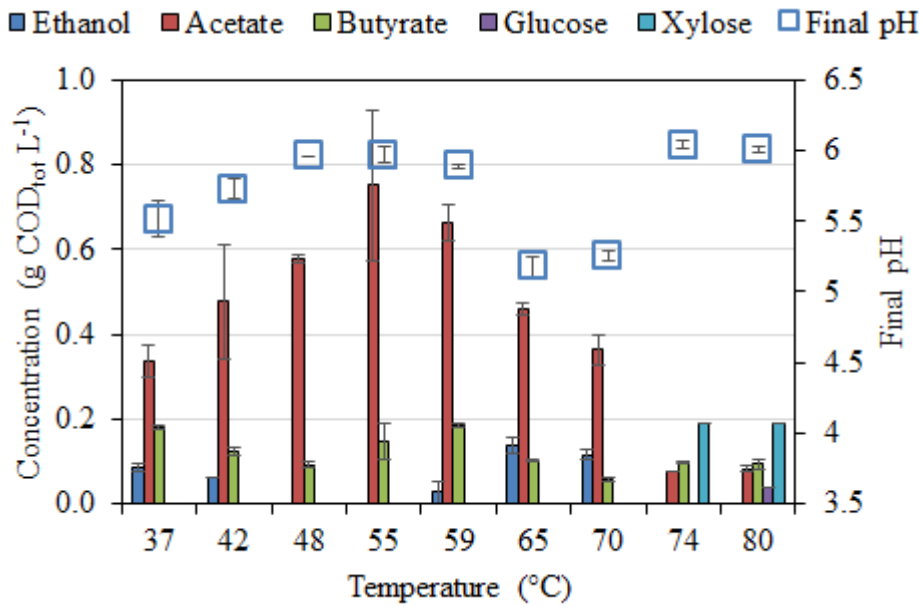
626

627

628

629

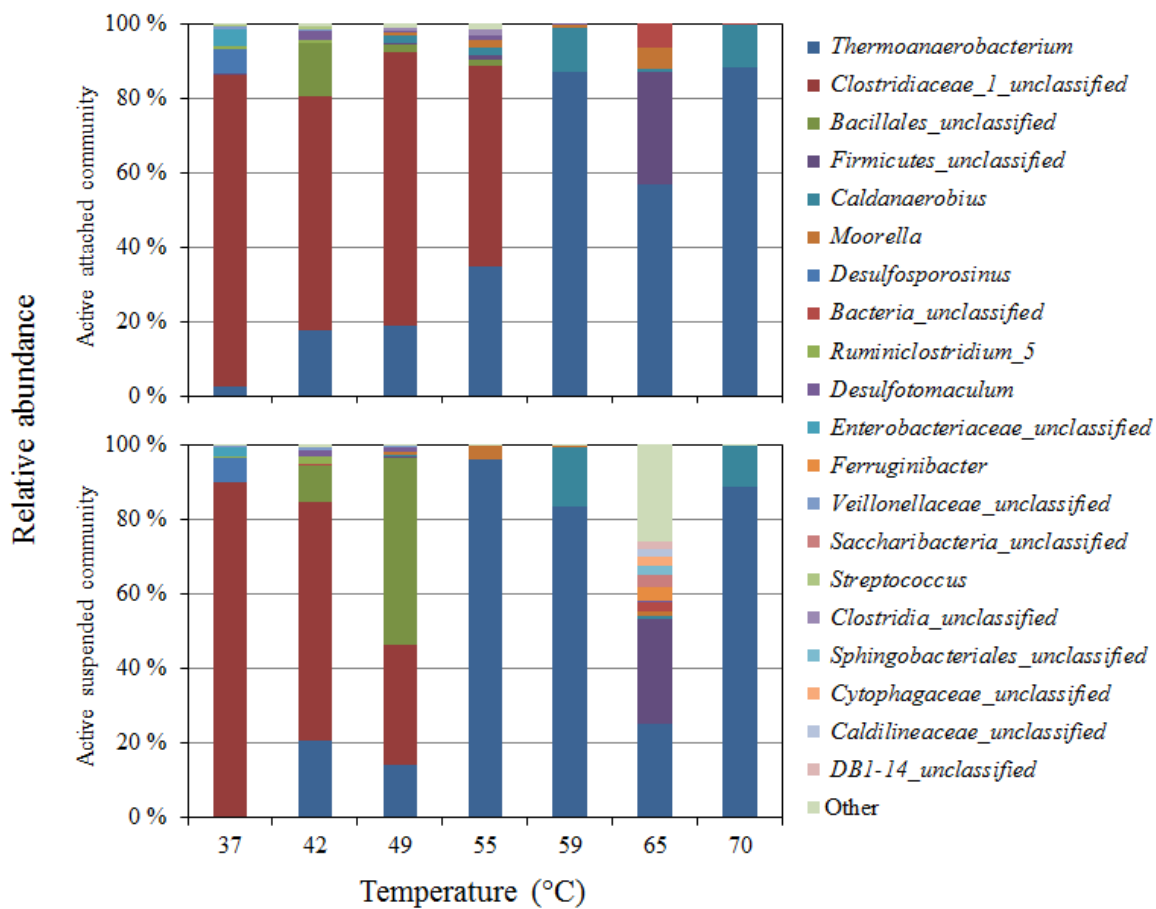
630 **Figure 2** – Concentration of detected sugars, volatile fatty acids and alcohols (on primary y-axis)
 631 and pH (on secondary y-axis) after 111 h of incubation of thermomechanical pulping wastewater at
 632 various temperatures (from 37 to 80 °C) using thermophilic biofilm-containing activated carbon as
 633 inoculum. Error bars refer to the standard deviations of the duplicates.
 634



635
 636
 637
 638
 639
 640
 641
 642
 643
 644

645 **Figure 3** – Relative abundance of the active genera resulting from MiSeq sequencing of the partial
 646 16S rRNA (transcribed to 16S cDNA) on microbiological samples obtained from the biofilm-
 647 containing activated carbon (attached) and from the liquid medium (suspended) after batch
 648 incubation with thermomechanical pulping wastewater at various temperatures (from 37 to 70 °C).
 649 The microbial genera are listed in order of relative abundance. Samples at 74 and 80 °C could not
 650 be analysed due to the low RNA concentration present in the samples.

651



652

653

654

655

656

657 **Table 1** - Composition of the thermomechanical pulping wastewater used in this study

Parameter	Concentration (mg L⁻¹)
Total solids	3771 ± 10
Volatile solids	2452 ± 8
Total COD	3352 ± 82
Soluble COD	3289 ± 54
Total nitrogen	< 10
Total PO ₄ ³⁻ -P	2.8
Acetate	< 30
Furfural	< 10
Glucose	43 (± 2)
Xylose	38 (± 0)

658

659

660

661

662

663

664

665

666

667 **Table 2** - Maximum and final hydrogen yield obtained from batch incubation of thermomechanical
 668 pulping wastewater at various temperatures (from 37 to 80 °C) using thermophilic biofilm-
 669 containing activated carbon as inoculum

Temperature (°C)	H ₂ yield (mmol H ₂ g ⁻¹ COD _{tot} supplied)		H ₂ yield (mmol H ₂ g ⁻¹ COD _{tot} consumed)	Time required for maximum H ₂ yield (h)
	Maximum	Final	Final	
37	3.2 (± 0.1)	1.4 (± 0.1)	1.9 (± 0.2)	23
42^a	1.5	0.6	1.3	63
48	0.6 (± 0.1)	0.1 (± 0.0)	0.1 (± 0.0)	18
55	0.4 (± 0.1)	0.0 (± 0.0)	0.0 (± 0.0)	12
59	1.7 (± 0.8)	0.6 (± 0.3)	0.9 (± 0.5)	18
65	3.7 (± 0.4)	1.8 (± 0.2)	2.6 (± 0.3)	36
70	3.6 (± 0.1)	3.6 (± 0.1)	4.9 (± 0.4)	90
74	0.1 (± 0.0)	0.1 (± 0.0)	0.2 (± 0.0)	n.a. ^b
80	0.0 (± 0.0)	0.0 (± 0.0)	0.0 (± 0.0)	n.a.

670 ^a Hydrogen was produced only in one of the duplicate tubes;

671 ^b Not applicable.

672

673

674

675

676

677

678

679 **Table 3** - COD_{tot} balances after incubation of thermomechanical pulping wastewater at various
 680 temperatures (from 37 to 80 °C) using thermophilic biofilm-containing activated carbon as
 681 inoculum

Temperature (°C)	Final COD_{tot} measured^a (g L⁻¹)	Final COD_{tot} estimated^b (g L⁻¹)	Difference (measured – estimated)	COD_{tot} removal (%)^c
37	0.79 (± 0.00)	0.60 (± 0.04)	0.19 (± 0.04)	72.5
42	0.58 (± 0.23)	0.66 (± 0.12)	-0.08 (± 0.11)	79.7
48	0.70 (± 0.01)	0.67 (± 0.00)	0.03 (± 0.02)	75.7
55	0.82 (± 0.14)	0.90 (± 0.22)	-0.07 (± 0.08)	71.2
59	0.84 (± 0.03)	0.88 (± 0.01)	-0.04 (± 0.04)	70.7
65	0.80 (± 0.04)	0.70 (± 0.03)	0.10 (± 0.00)	72.0
70	0.73 (± 0.10)	0.54 (± 0.03)	0.20 (± 0.07)	74.3
74	0.88 (± 0.06)	0.37 (± 0.00)	0.51 (± 0.07)	69.4
80	0.62 (± 0.06)	0.41 (± 0.02)	0.21 (± 0.05)	78.4

682 ^a Data obtained by measurement according to the standard procedure; the initial COD_{tot} was 2.86 g L⁻¹;

683 ^b Data obtained by the sum of the COD_{tot} equivalents (Eq. 1) of organic compounds measured in the liquid
 684 phase;

685 ^c Calculated from COD_{tot} measured.

686

687

688

689

690

691 **Table 4** - Association of the six most abundant 16S rRNA gene sequences to species collected in
 692 the GenBank

Family	Genus and species^a	Accession number	Matching sequence^b	Similarity (%)^c
<i>Thermoanaerobacteraceae</i>	<i>Thermoanaerobacterium thermosaccharolyticum</i>	JX984971	474-765	99
<i>Clostridiaceae</i>	<i>Clostridium</i> sp.	AY548785	450-741	99
<i>Bacillaceae</i>	<i>Bacillus coagulans</i>	MF373392	512-803	100
<i>Bacillaceae</i>	<i>Calditerricola yamamurae</i>	NR_112684	529-820	92
<i>Thermoanaerobacteraceae</i>	<i>Caldanaerobius</i> sp.	LC127102	482-773	99
<i>Thermoanaerobacteraceae</i>	<i>Moorella thermoacetica</i>	CP017237	145404-145695	100

693 ^a Closest cultured species in GenBank;

694 ^b Section of the 16S rRNA gene (in bp) matching the sequence obtained by MiSeq analysis;

695 ^c Percentage of identical nucleotide pairs between the 16S rRNA gene sequence and the closest cultured
 696 species in GenBank.

697

698

699

700

701

702

703

704

705 **Supporting material**

706 **Figure S1** – Carbon dioxide yield profiles (a) and acetate yield after 111 h of incubation (b)
707 obtained in the non-inoculated incubation of thermomechanical pulping wastewater at 37, 55 and 70
708 °C. Hydrogen was not detected at any of the temperatures tested. Error bars refer to the standard
709 deviations of the duplicates.

710 **Figure S2** – Adsorption of VFAs on activated carbon. Acetate and butyrate concentration before
711 and after 111 h of incubation with fresh activated carbon at 42, 65 and 80 °C. The initial
712 concentration of VFAs was chosen hypothesizing that only 40% of the 2.86 g COD_{tot} L⁻¹ was
713 removed through dark fermentation, and equally distributing the remaining 1.71 g COD_{tot} L⁻¹
714 between acetate and butyrate. Error bars refer to the standard deviations of the duplicates.

715

716 **Figure S3** – Carbon dioxide yield from batch incubation of thermomechanical pulping wastewater
717 at various temperatures (from 37 to 80 °C) using thermophilic biofilm-containing activated carbon
718 as inoculum. Error bars refer to the standard deviations of the duplicates.

Figure S1 – Carbon dioxide yield profiles (a) and acetate yield after 111 h of incubation (b) obtained in the non-inoculated incubation of thermomechanical pulping wastewater at 37, 55 and 70 °C. Hydrogen was not detected at any of the temperatures tested. Error bars refer to the standard deviations of the duplicates.

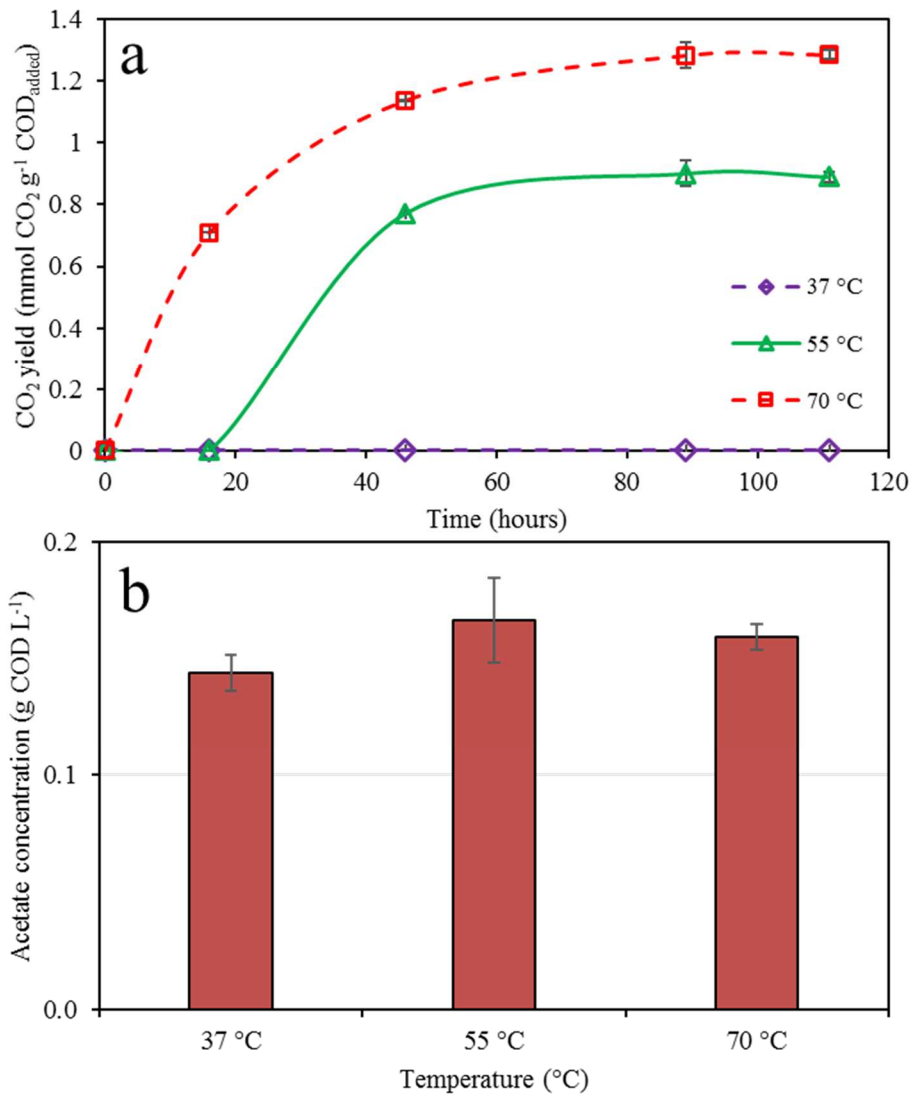


Figure S2 – Adsorption of VFAs on activated carbon. Acetate and butyrate concentration before and after 111 h of incubation with fresh activated carbon at 42, 65 and 80 °C. The initial concentration of VFAs was chosen hypothesizing that only 40% of the 2.86 g COD_{tot} L⁻¹ was removed through dark fermentation, and equally distributing the remaining 1.71 g COD_{tot} L⁻¹ between acetate and butyrate. Error bars refer to the standard deviations of the duplicates.

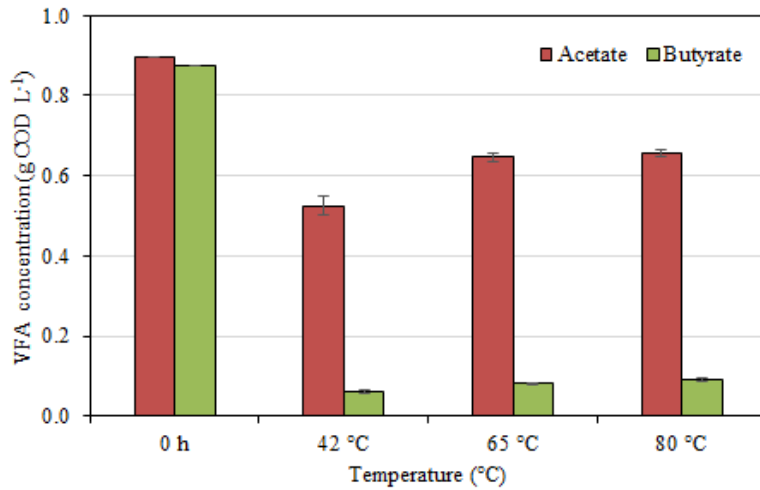


Figure S3 – Carbon dioxide yield from batch incubation of thermomechanical pulping wastewater at various temperatures (from 37 to 80 °C) using thermophilic biofilm-containing activated carbon as inoculum. Error bars refer to the standard deviations of the duplicates.

